PbTe/PbSnTe heterostructures as analogs of topological insulators

Ryszard Buczko and Łukasz Cywiński

Institute of Physics, Polish Academy of Sciences, Aleja Lotników 32/46, PL 02-668 Warszawa, Poland

We investigate theoretically the PbTe/$Pb_{1-x}Sn_x$Te heterostructure grown in the [111] direction, specifically a quantum wall (potential step of width d) of PbTe embedded in $Pb_{1-x}Sn_x$Te. For x large enough to lead to band inversion and for large d, there are well-known gapless interface states associated with four L valleys. We show that for $d \approx 10$ nm, the three pairs of states from oblique valleys strongly couple and become gapped with a gap ~ 10 meV. On the other hand, the interface states from the [111] valley are essentially uncoupled, and they retain their helical character, remaining analogous to states at surfaces of thin layers of three-dimensional topological insulators. This opens up a possibility of studying the physics of two-dimensional helical Dirac fermions in heterostructures of already widely studied IV-VI semiconductors.

I. INTRODUCTION

Much attention has been recently devoted to topological insulators (TIs), materials in which the topology of the bulk band structure guarantees the existence of robust (against nonmagnetic disorder) spin-nondegenerate (helical) edge/surface states.[1,2] TIs are essentially a subclass of narrow-gap semiconductors since their band gaps must be smaller than the typical energy scale of relativistic corrections to their band structures (<1 eV). In fact, the first two-dimensional (2D) TI was realized[3] in a quantum well of HgTe/HgCdTe, i.e., a heterostructure based on well-known compounds of narrow-gap semiconductors. Helical edge modes have also been recently reported in a heterostructure of InAs/GaSb.[4]

Part of the interest in TIs stems from the fact that they represent a new topological phase of noninteracting electrons: the TI character of a material is its bulk property, nontrivially encoded in the wave functions of the occupied (valence-band) states. However, it is the presence of the helical edge/surface states which leads to observable consequences. In three-dimensional strong (weak) TIs, they consist of an odd (even) number of spin-nondegenerate Dirac cones,[5] and many interesting effects have been predicted to occur when these states become gapped due to a perturbation,[1,2] e.g., due to proximity to a superconductor[6] or a ferromagnet.[7,8] The superconducting-proximity effect was predicted to lead to the creation of Majorana excitations at the surface of a TI[6] while covering the surface with a magnetic insulator was predicted to lead to new magnetoelectric effects.[7,8] By now many materials have been shown to be 3D TIs (see Ref. 1 and references therein) with Bi_2Se_3[9] and Bi_2Te_3[10] gathering the most attention due to the feature of having a single Dirac cone at the surface. Despite recent progress in the gating of thin layers of Bi_2Se_3,[11–13] it would be desirable to investigate the helical surface states in a well-known semiconductor system for which the growth and nanostructure processing are already mastered. One such platform is strained bulk HgTe.[14] In this article we propose to focus on heterostuctures of compound semiconductors from the IV-VI lead chalcogenide family, (Pb,Sn)Te.[15]

The superlattices of PbTe/$Pb_{1-x}Sn_x$Te (with $x \leqslant 0.18$) were thoroughly characterized.[16] Due to the huge dielectric constant of PbTe, mesoscopic structures of PbTe/PbEuTe

exhibit very robust ballistic transport properties.[17–19] Both Mn and Eu can be incorporated into PbTe, and exchange coupling between their spins and the band carriers was studied.[20] Furthermore, there exist heterostructures of PbTe and europium chalcogenides,[21,22] such as EuSe and EuTe, which are magnetic semiconductors with rich phase diagrams. Finally, a superconducting proximity effect has been recently shown to exist at In-PbTe junctions.[23] All these features suggest that IV-VI-based heterostructures, if they host gapless helical states, could be good candidates for investigations of phenomena related to TIs.

When changing the Sn content in a $Pb_{1-x}Sn_x$Te alloy, band inversion between the topmost valence band and the lowest conduction band occurs at $x \approx 0.37$. In an unstrained sample this happens simultaneously at the four L points at the edges of the Brillouin zone. Since the topological class of the band structure changes at the instances of local band gap closing[24] after an even number of local band inversions, this class remains the same. In fact, both PbTe and PbSnTe are in a topologically trivial class[5] although very recently it was argued[25] that SnTe is a topological crystalline insulator,[26] i.e., that it supports an even number of surface states for specific surface orientations. However, we focus here on the *mutual* band inversion between PbTe and PbSnTe, which leads to the existence of interfacial helical states, predicted theoretically 25 years ago.[27–30]

Such an interface of PbTe and $Pb_{1-x}Sn_x$Te, at which four Dirac cones appear, is analogous to the surface of a weak TI. Recent research on weak TIs suggests that these cones are in fact protected against time-reversal invariant perturbations as long as these are not periodic and commensurate with the lattice spacing,[31,32] a situation which is rather improbable at an epitaxial interface of two materials with the same lattice structure. It would, however, be even more interesting if one could obtain a single gapless helical state at an interface. As we show in this article, this can be instituted via a confinement effect in a properly designed PbTe/$Pb_{1-x}Sn_x$Te heterostructure grown in the [111] direction. This happens due to an anisotropic energy structure near the four L points, leading to a much stronger coupling of oblique valley states from opposite interfaces compared to the [111] valley along the growth direction. Note that a similar coupling opens up a

gap in a thin layer of a TI.[33–36] With a proper choice of strain, composition, and layer width, we obtain practically gapless helical states for the [111] valley with Dirac points located in the finite width-induced gap in the remaining three valleys.

The paper is organized in the following way. In Sec. II we describe the $\mathbf{k} \cdot \mathbf{p}$ Hamiltonian at the L-point band extrema in PbSnTe, and we note its close relation to the $\mathbf{k} \cdot \mathbf{p}$ Hamiltonian describing the states at the Γ point in Bi$_2$Se$_3$-type materials. In Sec. III we review the properties of helical states existing at the PbTe/Pb$_{1-x}$Sn$_x$Te interface, and we reexpress some known results[27–30] in a manner that shows their complete analogy with the surface states of TIs. Then, in Sec. IV we present the main results of the paper, the calculation of the electronic structure of a finite-width PbTe/Pb$_{1-x}$Sn$_x$Te heterostructure. There we present our prediction that in a properly designed heterostructure, one can have a practically gapless single Dirac cone with its Dirac point located in the gaps of the states from the other valleys. Finally, in Sec. V we discuss a few practical issues related to the experimental realization of the proposed heterostructure.

II. THE HAMILTONIAN

The electronic states near the L-point extrema in Pb$_{1-x}$Sn$_x$Te are described by Dimmock's Hamiltonian.[15,16] Since we focus on heterostructures grown in the [111] direction, we choose the z axis parallel to [111]. The Hamiltonian in the basis of $\frac{1}{\sqrt{2}}(X - iY)|\uparrow\rangle$, $\frac{1}{\sqrt{2}}(X + iY)|\downarrow\rangle$, $\frac{1}{\sqrt{2}}(S_X - iS_Y)|\uparrow\rangle$, and $\frac{1}{\sqrt{2}}(S_X + iS_Y)|\downarrow\rangle$ (where $S_{X,Y}$ transform like X,Y but do not change sign under reflection) is then given by

$$\hat{H} = \epsilon(\mathbf{k}) + \begin{pmatrix} \mathcal{M}(\mathbf{k}) & \hat{\sigma} \cdot \mathbf{Q} \\ \hat{\sigma} \cdot \mathbf{Q} & -\mathcal{M}(\mathbf{k}) \end{pmatrix} + \hat{H}_S, \quad (1)$$

where $\epsilon(\mathbf{k}) = V(x) + D_1 k_z^2 + D_2 k_\perp^2$, $\mathcal{M}(\mathbf{k}) = \Delta(x) + B_1 k_z^2 + B_2 k_\perp^2$, and $\mathbf{Q} = \hat{\mathbf{P}}_0 \cdot \mathbf{k}$. For the [111] valley, $\hat{\mathbf{P}}_0$ is a matrix with $(v_\perp, v_\perp, v_\parallel)$ on the diagonal. We stress that a realistic large ratio of $v_\perp/v_\parallel$ is crucial for our considerations. For remaining oblique valleys we replace $\hat{\mathbf{P}}_0$ with $\hat{\mathbf{P}} = \hat{\mathbf{S}}\hat{\mathbf{P}}_0\hat{\mathbf{S}}^{-1}$, where $\hat{\mathbf{S}}$ is a transformation matrix between the coordinate systems associated with the oblique valley $\{\hat{\mathbf{e}}_{\alpha'}\}$, with $\hat{\mathbf{e}}_{z'}$ along the valley direction, and $\{\hat{\mathbf{e}}_\alpha\}$, with $\hat{\mathbf{e}}_z$ along the growth axis: $(\hat{\mathbf{e}}_{x'}, \hat{\mathbf{e}}_{y'}, \hat{\mathbf{e}}_{z'}) = (\hat{\mathbf{e}}_x, \hat{\mathbf{e}}_y, \hat{\mathbf{e}}_z) \cdot \hat{\mathbf{S}}$.

We take $\Delta(x) = 0.095 - 0.26x$ eV, corresponding to the gap inversion at $x_c \approx 0.37$, and $V(x) = 0.125x$ eV.[16] For the remaining parameters we take $D_{1(2)} = 1.65(9.25)$ eV Å^2, $B_{1(2)} = 6.15(49.35)$ eV Å^2, $v_\parallel = 1.44$ eV Å, and $v_\perp = 4.76$ eV Å, and we neglect their composition dependence which is, if any, very weak in the considered regime of $x < 0.5$. Fitting of the Hamiltonian parameters to the results of nuclear-magnetic-resonance[37] measurements in Pb$_{1-x}$Sn$_x$Te with x up to 0.6 showed no changes in the $v_\perp$ or $v_\parallel$ parameters while the x dependence of $B_{1(2)}$ and $D_{1(2)}$ was inferred to be very weak. In other works,[38] a constant $v_\perp$ was inferred for x up to 0.16 while $v_\parallel$ was seen to change by an amount which extrapolates to about a 16% change for $x = 0.46$ compared to PbTe. Experimental data on the $v_\perp/v_\parallel$ ratio collected in Ref. 39 also suggest a very weak dependence of these parameters on the Sn content up to $x \approx 0.5$.

The strain described by tensor $\hat{\epsilon}$ is accounted for by $\hat{H}_S = \text{diag}\{D_d^c \text{Tr}\hat{\epsilon} + D_u^c \epsilon_{zz}, D_d^v \text{Tr}\hat{\epsilon} + D_u^v \epsilon_{zz}\}$ in which the two entries correspond to 2×2 blocks. Note that $\hat{H}_S$ gives strain-dependent corrections to Δ and V. The acoustic-deformation potentials are taken again as composition independent: $D_d^c = -1.09$ eV, $D_d^v = -2.23$ eV, $D_u^c = 2.07$ eV, and $D_u^v = 2.62$ eV.[16] The lattice constants of PbTe (SnTe) are taken as $a_0 = 6.454$ Å(6.313 Å).

The above Hamiltonian is written in a form which allows one to immediately see that after a basis reordering it becomes the same as the recently studied model $\mathbf{k} \cdot \mathbf{p}$ Hamiltonian describing the states near the Γ point in the Bi$_2$Se$_3$ family of materials.[40] There, the TI phase occurs[33,40] when $\Delta \cdot B_{1,2} < 0$, i.e., when the conduction and valence bands at the Γ point become inverted. As mentioned before, in unstrained Pb$_{1-x}$Sn$_x$Te the inversion occurs simultaneously at four L points, and the bulk phase remains topologically trivial.

III. HELICAL NATURE OF INTERFACE STATES

We first analyze interface bound states (IBS) localized at two decoupled heterointerfaces of a very wide PbTe/Pb$_{1-x}$Sn$_x$Te heterostructure grown in the [111] direction. We assume that for $|z| < d/2$ we have the values of $\Delta > 0$ and V, corresponding to PbTe, while $\Delta' < 0$ and V' correspond to Pb$_{0.54}$Sn$_{0.46}$Te. From the point of view of band lineup, this structure is in fact a finite-width potential step—a quantum *wall* (QWa) instead of a quantum *well* (QWe).

We use the effective-mass approximation and replace k_z by $-i\partial/\partial z$ in Eq. (1). As long as the intervalley coupling (due to alloy disorder or atomic-scale-interface reconstruction) can be neglected, the presence of mutual-band inversion at the interfaces guarantees the existence of helical Dirac-like IBS.[27,30] The dispersion and the spin structure of IBS is insensitive to the exact profile of the interface[27,30] with only the z dependence of wave functions being affected in the region of interdiffusion. For simplicity we assume an abrupt interface[28,29,41] and use the boundary conditions of continuity of the wave function and its derivative (the latter only when we consider nonzero k^2 terms). Note that these boundary conditions are sufficient in the case when, as we assume, the $\mathbf{k} \cdot \mathbf{p}$ Hamiltonian's parameters $v_\perp$, $v_\parallel$, $D_{1,2}$, and $B_{1,2}$ are the same for both compounds.

Since our numerical calculations show that for realistic parameters the k^2 terms are of minor quantitative importance, we present much simpler analytical results obtained by neglecting them. We also focus on results for the [111] valley, which we label with superscript α (with β denoting the oblique-valley results). The energies of the IBS are $E_\pm^\alpha(k_\perp) = E_0 \pm v_\perp k_\perp \frac{\mathcal{D}}{\Delta - \Delta'}$, where $\mathcal{D}^2 = (\Delta - \Delta')^2 - (V - V')^2$ and $E_0 = \frac{\Delta V' - V\Delta'}{\Delta - \Delta'}$. (In oblique valleys the dispersion is, of course, anisotropic in $\mathbf{k}_\perp$.) The eigenvectors are the 4-spinors $\hat{\psi}_\pm^{L/R}(\mathbf{k}_\perp)$ with L/R denoting the left ($z = -d/2$) and the right ($z = d/2$) interfaces, respectively, multiplied by appropriate functions $f_\pm^{L/R}(z)$ describing the exponential decay away from a given interface. The inverse-decay lengths are given by

$$\chi_\pm^\alpha = \frac{1}{v_\parallel}\left(\mathcal{D}\frac{\Delta}{\Delta - \Delta'} \pm \eta v_\perp k_\perp\right) \quad (2)$$

in the middle layer and $\chi'_\pm = \chi_\pm(\Delta \leftrightarrow \Delta')$ outside with $\eta \equiv (V - V')/(\Delta - \Delta')$. Let us note that in the oblique valley case $\chi_\pm^\beta$ acquire an imaginary part at finite $\mathbf{k}_\perp$; however, what is crucial is the fact that at $k_\perp = 0$, χ_0^β is given by Eq. (2) with $v_\parallel$ replaced by $\frac{1}{3}\sqrt{8v_\perp^2 + v_\parallel^2}$.

The two-dimensional subspaces of IBS at the two interfaces are spanned by 4-spinors $\{\hat{\phi}_\uparrow^{L/R}, \hat{\phi}_\downarrow^{L/R}\}$ for which the subscripts signify that their components correspond to well-defined spin states although they remain linear combinations of different orbitals. Defining $\gamma \equiv \arctan\sqrt{(1 + \eta)/(1 - \eta)}$, we can write them as $\hat{\phi}_\uparrow^{L/R} = [\mp i\cos\gamma, 0, \sin\gamma, 0]^T$ and $\hat{\phi}_\downarrow^{L/R} = [0, \pm i\cos\gamma, 0, \sin\gamma]^T$. Using these basis states, we can write the solutions of the 4-spinor parts of the IBS: $\hat{\psi}_\pm^L(\mathbf{k}_\perp) = (\pm i\hat{\phi}_\uparrow^L + e^{i\theta}\hat{\phi}_\downarrow^L)/\sqrt{2}$ and $\hat{\psi}_\pm^R(\mathbf{k}_\perp) = (\hat{\phi}_\uparrow^R \pm ie^{i\theta}\hat{\phi}_\downarrow^R)/\sqrt{2}$, where $e^{i\theta} = (k_x + ik_y)/k_\perp$.

The helical nature of these states can be seen by calculating the expectation values of spin operators: $\langle\hat{\psi}_\pm^L|\hat{\sigma}_x|\hat{\psi}_\pm^L\rangle = \mp\cos 2\gamma \sin\theta$ and $\langle\hat{\psi}_\pm^L|\hat{\sigma}_y|\hat{\psi}_\pm^L\rangle = \pm\cos 2\gamma \cos\theta$, i.e., the spin vector is perpendicular to $\mathbf{k}_\perp$, pointing clockwise (anticlockwise) for the negative (positive) energy branch. The pattern on the R interface is reversed. More generally,[42] we can write an effective surface Hamiltonian in the $\{\hat{\phi}_\uparrow^{L/R}, \hat{\phi}_\downarrow^{L/R}\}$ basis:

$$\hat{H}_{\text{surf}}^{L/R} = \pm v_\perp \frac{\mathcal{D}}{\Delta - \Delta'}(\tilde{\sigma}_x k_y - \tilde{\sigma}_y k_x) \qquad (3)$$

with the $\tilde{\sigma}$ Pauli matrices operating in the respective two-dimensional spaces. Let us remark that the spin pattern for states from the oblique valleys is more complicated with nonzero out-of-plane $\langle\hat{\sigma}_z\rangle$ polarization.

All these results show complete analogy with the surface states in TIs such as Bi_2Se_3.[40] The difference is the existence of four pairs of IBS with the states from all the valleys coexisting at a given energy in the bulk gap, showing that the PbTe/Pb$_{1-x}$Sn$_x$Te heterointerface is analogous to the surface of a weak TI.

IV. THE EFFECT OF FINITE QUANTUM-WALL WIDTH

We assume that the lattice mismatch between PbTe and Pb$_{0.54}$Sn$_{0.46}$Te is shared in the 4 : 1 ratio between the two materials (i.e., assuming a common lattice constant corresponding to the 0.37 content of Sn). This requires an engineering of strain distribution by, e.g., the choice of a substrate. If we neglect the k^2 terms, the calculation is fairly straightforward.[28,29,41] With the k^2 terms and for a general valley direction, we have to resort to solving the problem numerically.

In Fig. 1 we show the energy dispersion of the [111]-valley states formed in the QWa. For both widths of $d = 12$ and

FIG. 1. (Color online) The solid line is the dispersion of the [111]-valley interface bound states for the PbTe/Pb$_{0.54}$Sn$_{0.46}$Te quantum wall grown in the [111] direction with PbTe widths d of 12 and 100 nm (undistinguishable), plotted as a function of the in-plane k vector. The dashed lines are the bulk band edges for Pb$_{0.54}$Sn$_{0.46}$Te. (The band edges of PbTe are outside of the shown energy region.) There is a gap of 0.2 meV opened at the Dirac point for $d = 12$ nm (see Fig. 3).

FIG. 2. (Color online) The solid line is the dispersion of the [$\bar{1}$11]-valley IBS for the PbTe/Pb$_{0.54}$Sn$_{0.46}$Te quantum wall with a PbTe width d of (a) 100 nm and (b) 12 nm. The dashed (dotted) lines are the bulk band edges for Pb$_{0.54}$Sn$_{0.46}$Te (PbTe). The gap of ~10 meV opens for $d = 12$ nm.
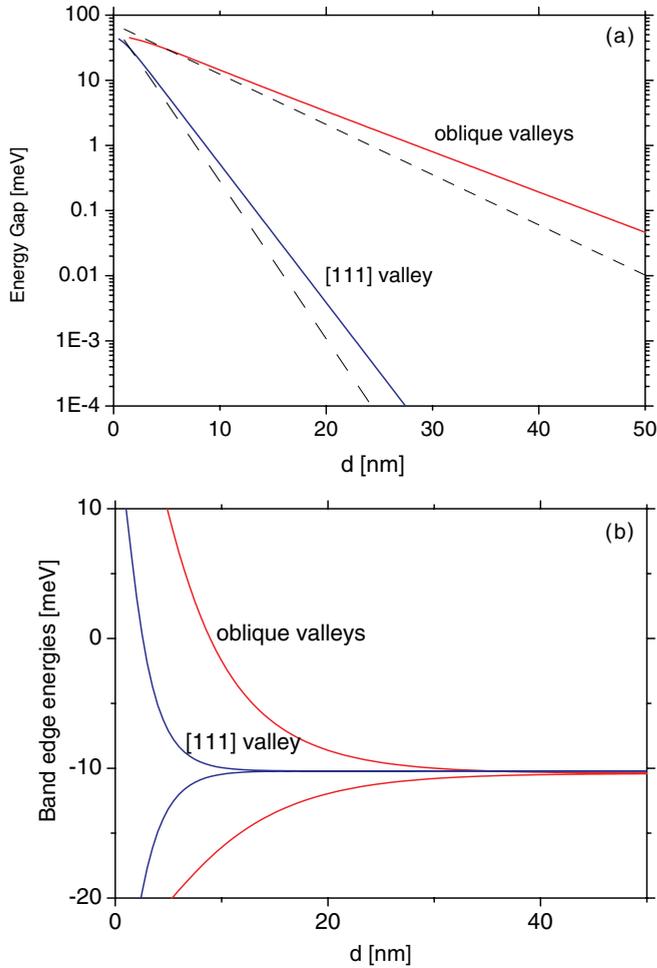
FIG. 3. (Color online) (a) The energy gaps of the IB-derived states from the [111] valley and the three oblique valleys. The solid lines are the results of an exact calculation while the dashed lines are obtained with Eq. (4), which neglects the k^2 terms in the Hamiltonian. (b) Band-edge energies for the IB-derived states. The Dirac point of the [111]-valley states is located in the gap of the states from the remaining valleys.

100 nm, the IBS from the two interfaces remain practically uncoupled: the gap opened for $d = 12$ nm is only ≈ 0.2 meV. On the other hand, as we show in Fig. 2 with decreasing d, a sizable gap opens for the interface bound (IB) derived states (formed due to the coupling of IBS from the opposite interfaces) in the oblique valleys, and it is ~ 10 meV for $d = 12$ nm. As shown in Fig. 3(a), the gaps $E_g^{\alpha/\beta}$ are visibly different. Thus, for most practical purposes (e.g., for experiments done at temperatures ~ 1 K) in a structure with $d \approx 10$ nm, the dispersion of the states from the [111] valley can be considered gapless while the states from the oblique valleys are gapped. Let us also stress that at energies $|E_{\pm}(\mathbf{k}_{\perp}) - E_0| \gg E_g$, the eigenstates are essentially the L/R-interface bound states (the description in terms of massive Dirac fermions[35] is relevant only at small $\mathbf{k}_{\perp}$). Furthermore, as shown in Fig. 3(b) for the chosen QWa, the [111]-valley states are in the gap of the oblique valley solutions so that disorder with a typical energy scale smaller than this gap cannot mix the states from the [111] valley with the others. Thus, for an epitaxial interface of good

quality we expect that the above-described system is basically equivalent to a layer of material such as Bi_2Te_3 or Bi_2Se_3 with the only difference being the smaller size of the gap within which the surface states exist (~ 10 meV vs ~ 0.3 eV).

The above results can be understood using a calculation with the k^2 terms neglected and d assumed to be large. We orthogonalize the IBS and form their symmetric and anti-symmetric combinations, approximating the exact solutions in the large-d limit. We calculate the gap by evaluating the matrix elements of the QWa Hamiltonian between them. The d dependence of $E_g^{\alpha,\beta}$ comes from exponential decay of the IBS in the step region, described by inverse lengths $\chi_0^{\alpha,\beta}$ (calculated for $k_{\perp} = 0$) given in Eq. (2) and below. In this way we obtain the band gaps (see also Ref. 28):

$$E_g^{\alpha/\beta} = 4\mathcal{D}^2 \frac{|\Delta\Delta'|}{(\Delta - \Delta')^3} \exp(-\chi^{\alpha/\beta}d). \quad (4)$$

The predictions of this formula agree well with the results of the full calculation shown in Fig. 3(a).

V. DISCUSSION

The above choice of a heterostructure was dictated by the strain dependence of the energies of band extrema in $Pb_{1-x}Sn_xTe$. As shown in Fig. 4 when the lattice constant of $Pb_{1-x}Sn_xTe$ is adjusted to the PbTe constant in a heterostructure grown in the [111] direction, with the realistic values of deformation potentials[16] we obtain that the gaps at the [111] L point and the remaining ones *do not overlap*. One can see then that in the $Pb_{1-x}Sn_xTe$ quantum well (with PbTe being the barrier), it is practically impossible (without applying a compressive strain) to obtain a Dirac point of the [111]-valley IBS within the gap of the oblique valley IB-derived states. For the QWa with material parameters adopted here, we only require a modest amount of additional tensile strain, which could be provided at low temperatures by BaF_2 substrate typically used for IV-VI compounds.[16] Additional tuning of
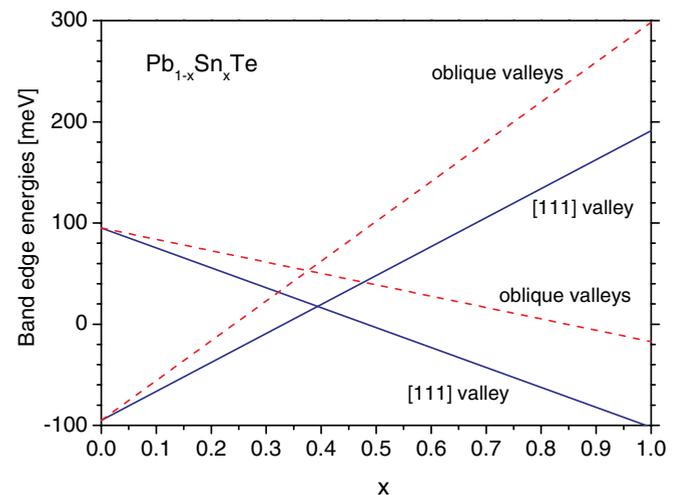
FIG. 4. (Color online) The energies of the extrema of the conduction and valence bands for the $Pb_{1-x}Sn_xTe$ lattice matched to PbTe (grown in the [111] direction), calculated using Eq. (1) as a function of x.

band-edge offsets can also be obtained by using quaternary alloys and replacing a fraction of Te with Se.

Note, however, that if band-inverted $Pb_{1-x}Sn_xTe$ itself possesses gapless surface states,[25] which would then appear at its interfaces with the substrate and with the gate covering the structure, then the choice of a compressively strained $Pb_{1-x}Sn_xTe/PbTe$ quantum well will be more experimentally practical. In such a case, apart from the IB-derived states we obtain also the "normal" quantum-well states with energies outside of the gap of $Pb_{1-x}Sn_xTe$. The behavior of gaps of IB-derived states as a function of d is analogous to the QWa case, and with the same strain distribution as used before, i.e., strain shared in a 4:1 ratio between PbTe and $Pb_{0.54}Sn_{0.46}Te$, the Dirac point of the [111]-valley states can be located in the gap of the remaining IB-derived states (and, of course, also in the gap of all the normal quantum-well states).

Let us note that a result qualitatively the same as shown in Fig. 4 can be obtained for $Pb_{1-x}Sn_xTe$ uniaxially strained in the [111] direction. The nonoverlapping of band gaps in the range of x corresponding to the inverted oblique valley and noninverted [111] valley implies that applying such a strain, as proposed in Ref. 5, cannot change $Pb_{1-x}Sn_xTe$ into a strong TI but into a topological semimetal.

Another possible practical obstacle in the investigation of helical states in the proposed structure is the issue of p-type self-doping[43] of $Pb_{1-x}Sn_xTe$ with $x > 0.2$. This is analogous to the situation in materials from the Bi_2Se_3 family, the members of which possess large bulk conductivities when as-grown (see, e.g., Ref. 44). At $x = 0.25$, holes were compensated by indium doping,[45] but it remains to be investigated how effective this would be at $x \sim 0.4$ as considered here.

VI. CONCLUSIONS

We have calculated the band structure of a heterostructure based on PbTe and band-inverted $Pb_{1-x}Sn_xTe$ in which PbTe forms a quantum wall of finite thickness d. The normal quantum-well states are then absent, and the localized solutions appear due to the mutual band inversion between the constituent materials. For very large d these solutions correspond to four pairs of Dirac cones located at the two interfaces.[27–30] As the QWa grown in the [111] direction is narrowed, these states become gapped due to the overlap of wave functions localized on the two interfaces. We have found that the opened gap is at least two orders of magnitude larger for states associated with three oblique valleys compared to the states from the [111] valley. Thus, after properly choosing the QWa composition, its width, and the strain distribution in it, one can obtain a practically gapless pair of helical Dirac states from the [111] valley with their Dirac points located in the gaps of the states from the other valleys. The IV-VI heterostructure can then serve as an analog of a thin layer of a strong topological insulator.

[1] M. Z. Hasan and C. L. Kane, Rev. Mod. Phys. **82**, 3045 (2010).

[2] X.-L. Qi and S.-C. Zhang, Rev. Mod. Phys. **83**, 1057 (2011).

[3] M. Konig, S. Wiedmann, C. Brune, A. Roth, H. Buhmann, L. W. Molenkamp, X.-L. Qi, and S.-C. Zhang, Science **318**, 766 (2007).

[4] I. Knez, R.-R. Du, and G. Sullivan, Phys. Rev. Lett. **107**, 136603 (2011).

[5] L. Fu and C. L. Kane, Phys. Rev. B **76**, 045302 (2007).

[6] L. Fu and C. L. Kane, Phys. Rev. Lett. **100**, 096407 (2008).

[7] X.-L. Qi, T. L. Hughes, and S.-C. Zhang, Phys. Rev. B **78**, 195424 (2008).

[8] A. M. Essin, J. E. Moore, and D. Vanderbilt, Phys. Rev. Lett. **102**, 146805 (2009).

[9] Y. Xia, D. Qian, D. Hsieh, L. Wray, A. Pal, H. Lin, A. Bansil, D. Grauer, Y. S. Hor, R. J. Cava *et al.*, Nat. Phys. **5**, 398 (2009).

[10] Y. L. Chen, J. G. Analytis, J.-H. Chu, Z. K. Liu, S.-K. Mo, X. L. Qi, H. J. Zhang, D. H. Lu, X. Dai, Z. Fang *et al.*, Science **325**, 178 (2009).

[11] J. G. Checkelsky, Y. S. Hor, R. J. Cava, and N. P. Ong, Phys. Rev. Lett. **106**, 196801 (2011).

[12] B. Sacepe, J. B. Oostinga, J. Li, A. Ubaldini, N. J. G. Couto, E. Giannini, and A. F. Morpurgo, Nat. Comm. **2**, 575 (2011).

[13] D. Kim, S. Cho, N. P. Butch, P. Syers, K. Kirshenbaum, S. Adam, J. Paglione, and M. S. Fuhrer, Nat. Phys., advance online publication, doi: 10.1038/NPHYS2286 (2012).

[14] C. Brüne, C. X. Liu, E. G. Novik, E. M. Hankiewicz, H. Buhmann, Y. L. Chen, X. L. Qi, Z. X. Shen, S. C. Zhang, and L. W. Molenkamp, Phys. Rev. Lett. **106**, 126803 (2011).

[15] G. Nimtz and B. Schlicht, in *Narrow-Gap Semiconductors*, Springer Tracts in Modern Physics Vol. 98, edited by G. Höhler (Springer-Verlag, Berlin, 1983), p. 1.

[16] M. Kriechbaum, K. E. Ambrosch, E. J. Fantner, H. Clemens, and G. Bauer, Phys. Rev. B **30**, 3394 (1984).

[17] G. Grabecki, J. Wróbel, T. Dietl, E. Janik, M. Aleszkiewicz, E. Papis, E. Kamińska, A. Piotrowska, G. Springholz, and G. Bauer, Phys. Rev. B **72**, 125332 (2005).

[18] G. Grabecki, J. Wróbel, T. Dietl, E. Janik, M. Aleszkiewicz, E. Papis, E. Kaminska, A. Piotrowska, G. Springholz, and G. Bauer, Phys. E (Amsterdam, Neth.) **34**, 560 (2006).

[19] K. A. Kolwas, G. Grabecki, S. Trushkin, J. Wróbel, M. Aleszkiewicz, Ł. Cywiński, T. Dietl, G. Springholz, and G. Bauer, e-print arXiv:1111.2433 (2011).

[20] T. Dietl, C. Śliwa, G. Bauer, and H. Pascher, Phys. Rev. B **49**, 2230 (1994).

[21] H. Kepa, G. Springholz, T. M. Giebultowicz, K. I. Goldman, C. F. Majkrzak, P. Kacman, J. Blinowski, S. Holl, H. Krenn, and G. Bauer, Phys. Rev. B **68**, 024419 (2003).

[22] R. T. Lechner, G. Springholz, T. U. Schülli, J. Stangl, T. Schwarzl, and G. Bauer, Phys. Rev. Lett. **94**, 157201 (2005).

[23] G. Grabecki, K. A. Kolwas, J. Wróbel, K. Kapcia, R. Puźniak, R. Jakieła, M. Aleszkiewicz, T. Dietl, G. Springholz, and G. Bauer, J. Appl. Phys. **108**, 053714 (2010).

[24] S. Murakami and S.-I. Kuga, Phys. Rev. B **78**, 165313 (2008).

[25] T. H. Hsieh, H. Lin, J. Liu, W. Duan, A. Bansil, and L. Fu, e-print arXiv:1202.1003 (2012).

[26]L. Fu, Phys. Rev. Lett. **106**, 106802 (2011).

[27]B. A. Volkov and O. A. Pankratov, JETP Lett. **42**, 178 (1985).

[28]V. Korenman and H. D. Drew, Phys. Rev. B **35**, 6446 (1987).

[29]D. Agassi and V. Korenman, Phys. Rev. B **37**, 10095 (1988).

[30]O. A. Pankratov, Semicond. Sci. Technol. **5**, S204 (1990).

[31]Z. Ringel, Y. E. Kraus, and A. Stern, e-print arXiv:1105.4351 (2011).

[32]R. S. K. Mong, J. H. Bardarson, and J. E. Moore, Phys. Rev. Lett. **108**, 076804 (2012).

[33]C.-X. Liu, H. J. Zhang, B. Yan, X.-L. Qi, T. Frauenheim, X. Dai, Z. Fang, and S.-C. Zhang, Phys. Rev. B **81**, 041307 (2010).

[34]J. Linder, T. Yokoyama, and A. Sudbø, Phys. Rev. B **80**, 205401 (2009).

[35]H.-Z. Lu, W.-Y. Shan, W. Yao, Q. Niu, and S.-Q. Shen, Phys. Rev. B **81**, 115407 (2010).

[36]W.-Y. Shan, H.-Z. Lu, and S.-Q. Shen, New J. Phys. **12**, 043048 (2010).

[37]C. R. Hewes, M. S. Adler, and S. D. Senturia, Phys. Rev. B **7**, 5195 (1973).

[38]G. Appold, R. Grisar, G. Bauer, H. Burkhard, R. Ebert, H. Pacher, and H. G. Häfele, in *Proceedings of the 14th International Conference on the Physics of Semiconductors*, edited by B. L. H. Wilson (Institute of Physics, Edinburgh, 1979), p. 1101.

[39]Y. S. He and A. D. C. Grassie, J. Phys. F **15**, 263 (1985).

[40]C.-X. Liu, X.-L. Qi, H. J. Zhang, X. Dai, Z. Fang, and S.-C. Zhang, Phys. Rev. B **82**, 045122 (2010).

[41]V. K. Dugaev and P. P. Petrov, Phys. Status Solidi B **184**, 347 (1994).

[42] Note that for $\cos 2\gamma = 0$, i.e., for $V = V'$, there is no real spin texture. What remains is the pseudospin texture described by Eq. (3), which still provides protection against elastic backscattering.

[43]L. V. Prokofievaa, Y. I. Ravich, D. A. Pshenay-Severin, P. P. Konstantinov, and A. A. Shabaldin, Semiconductors **44**, 712 (2010).

[44]N. P. Butch, K. Kirshenbaum, P. Syers, A. B. Sushkov, G. S. Jenkins, H. D. Drew, and J. Paglione, Phys. Rev. B **81**, 241301 (2010).

[45]D. R. Khokhlov, I. I. Ivanchik, S. N. Raines, D. M. Watson, and J. L. Pipher, Appl. Phys. Lett. **76**, 2835 (2000).